SAND2022-11792C

The Impact of Co-Located Clusters of Inverter-Based Resources on a Performance-Based Regulation Market Metric

Thad Haines
Sandia National Laboratories
Albuquerque, NM
jthaine@sandia.gov

Rachid Darbali-Zamora
Sandia National Laboratories
Albuquerque, NM
rdarbal@sandia.gov

Miguel Jiménez-Aparicio
Sandia National Laboratories
Albuquerque, NM
mjimene@sandia.gov

Felipe Wilches-Bernal
Sandia National Laboratories
Albuquerque, NM
fwilche@sandia.gov

***Abstract*—This paper demonstrates that a faster Automatic Generation Control (AGC) response provided by Inverter-Based Resources (IBRs) can improve a performance-based regulation (PBR) metric. The improvement in performance has a direct effect on operational income. The PBR metric used in this work was obtained from a California ISO (CAISO) example and is fully described herein. A single generator in a modified three area IEEE 39 bus system was replaced with a group of co-located IBRs to present possible responses using different plant controls and variable resource conditions. We shown how a group of IBRs that rely on variable resources may negatively affect the described PBR metric of all connected areas if adequate plant control is not employed. However, increasing the dispatch rate of internal plant controls may positively affect the PBR metric of all connected areas despite variable resource conditions.**

***Index Terms*—Automatic Generation Control, Performance-Based Regulation, Inverter-Based Resource**

I. Introduction

Standards and regulations require that power systems can provide adequate frequency response [1]. With more Distributed Energy Resources (DERs) such as solar photovoltaics (PV), wind turbine generators (WT), and battery energy storage systems (BESS) replacing conventional generation sources, new challenges related to their variable nature are introduced. These Inverter Based Resources (IBRs) allow faster control response compared to conventional generation sources. It is essential to coordinate and adequately manage IBRs to ensure appropriate system conditions for continuous operation.

Additionally, [1] encourages proper compensation of generation operators whose faster-ramping resources may provide more frequency regulation services than previously acknowledged. To that end, various Performance-Based Regulation (PBR) market techniques have emerged to more fairly compensate resources that are asked to do more work. As described in [2], existing approaches have been developed to address perceived area specific generation compensation shortfalls or to improve overall system efficiency.

Sandia National Laboratories is a multimission laboratory managed and operated by National Technology and Engineering Solutions of Sandia, LLC., a wholly owned subsidiary of Honeywell International, Inc., for the U.S. Department of Energy's National Nuclear Security Administration under contract DE-NA0003525. This research was supported by The U.S. Department of Energy's Grid Modernization Laboratory Consortium program.

This work utilized a cluster of co-located IBRs, termed a Flexpower plant, that consists of a solar PV plant, a WT, and a BESS connected to a shared power system bus. The Flexpower plant can provide frequency regulation to a power system as well as dispatch following support. Previously, the Flexpower plant has been shown to provide resource aware fast frequency regulation [3] and synthetic inertia [4] to a small power system. This paper presents the impact of a single Flexpower plant on a PBR market metric using a modified IEEE 39 bus system, two internal plant control approaches, and variable generation resources.

The rest of this paper is structured as follows: Section II describes the test system and models, Section III defines the PBR metric used in this work, Section IV provides information on the Automatic Generation Control (AGC) model and operation, Section V outlines the simulated test cases, Section VI reports simulation results, and Section VII provides conclusions.

II. Test System and Models

A. IEEE 39 Bus System

The IEEE 39 bus system has been widely used and modified for many power system focused papers [5]–[8]. The version of the IEEE 39 system for this work was modified from the MATLAB Simulink model described in [8]. The system consists of 39 buses, 10 steam based generators, and 18 loads. To simulate a multi-area system, three areas (North, East, and West) were defined. A one-line depiction of the system with defined areas is shown in Fig. 1.

Table I presents the total loads and exports of each area within the system. Both the North and West areas are exporting power while the East area is importing power. Table II describes system-wide generation resources and control by area. Only one generator per area receives an AGC dispatch signal. Other controlled generators respond to system conditions through turbine speed governors while one generator in each area acts as a constant power generation source. All conventional generators are equipped with exciters to manage voltage.

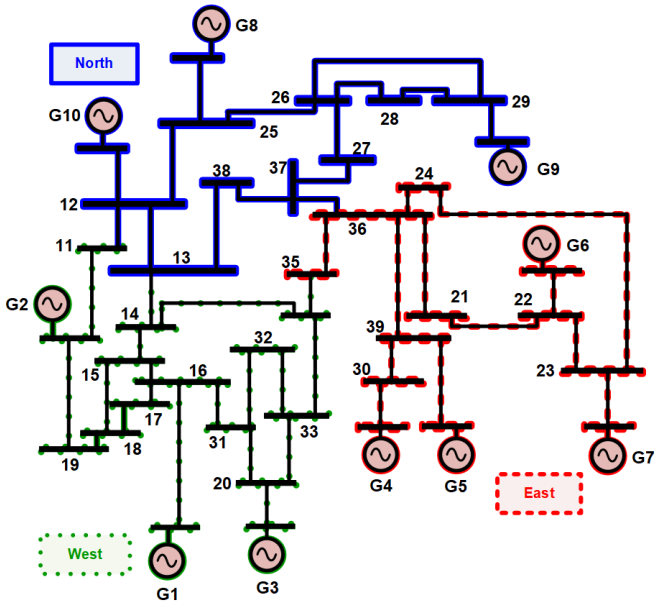

Fig. 1. One-line diagram of the multi-area IEEE 39 bus system.

A Flexpower plant is used to replace conventional generator G10 in the North area for Flexpower simulation cases. In other words, the Flexpower plant is connected to the system only when G10 is removed from the system. This is to demonstrate how a single Flexpower plant may perform within a system compared to conventional rotating-mass generation.

TABLE I
SYSTEM LOAD AND EXPORT CHARACTERISTICS BY AREA.

Area	Load [MW]	Export [MW]
North	1341	132
East	2107	-425
West	2367	293

B. Flexpower Plant

The Flexpower plant, defined as a group of co-located IBRs, used in this work contains a WT, PV plant, and a BESS. Table III presents the rated voltages, power ratings, as well as initial real and reactive power outputs for each device in the Flexpower plant. Further details about the device models are provided in the following subsections.

1) Photovoltaic Inverter: The model used for the photovoltaic inverter was adapted from [9]. It contains an average inverter model that controls real and reactive power via pulse width modulation signals that define the direct and quadrature current injections. An irradiance input allows the device to output rated power when irradiance is 1000 W/m^2. The irradiance input also limits the output of the device when the irradiance varies below the rated value.

2) Wind Turbine Generator: A Type-4 wind turbine model was used for the WT contained in the Flexpower plant. The model is described and validated in [10]–[12]. Real and imaginary current injections act as the grid interface for the

TABLE II
SYSTEM WIDE GENERATION RATING AND CONTROL DESCRIPTIONS. THE NORTH AREA CONTAINS G10 OR THE FLEXPOWER PLANT DEPENDING ON SIMULATION CASE.

Area	Source	Machine Base (MVA)	Control
West	G1	3000	-
	G2	1000	Governor
	G3	1000	AGC
East	G4	1000	Governor
	G5	520	-
	G6	1000	Governor
	G7	1000	AGC
North	G8	1000	-
	G9	1000	Governor
	G10	1000	AGC
	Flexpower		
	PV+WT	570	-
	BESS	100	AGC

TABLE III
FLEXPOWER GENERATION PARAMETERS.

Tech Type	Voltage (kV)	Power Rating (MVA)	Active Power Ref. (MW)	Reactive Power Ref. (MVAR)
PV	0.69	220	120	1
WTG	0.69	350	225	2
BESS	0.48	100	-30	0

WT to supply real or reactive power, respectively. The WT has blade pitch control to mechanically set the generated power and also contains functionality to directly control the inverter output to allow for faster set point changes. Similar to the PV model, the WT accepts a wind speed variable to limit the output of the device when wind speed is below its rated value.

3) Battery Energy Storage System: The BESS inverter was modeled similarly to the PV, but allows for power absorption and includes a state of charge (SOC) variable that defines the amount of energy the BESS may provide or absorb as described in [13]. However, for this particular simulation, capacity of the BESS was increased such that it would not encounter SOC issues over the course of a 15 minute simulation.

III. PERFORMANCE-BASED REGULATION METRIC

The performance-based regulation (PBR) metric used in this work was derived from a California ISO (CAISO) example [14]. The calculation is described later in this section, but essentially, the accuracy of a resources ability to follow an AGC dispatch is assessed for a market period of 15 minutes. The resulting accuracy value, or Performance Score (PS), is used by utilities to directly scale the price paid for an area's MW regulation, or 'mileage' as it is referred to in [15].

In this work, the PS is represented as a percentage calculated for both regulation up and regulation down commands. The direction of the regulation classification is based on a set point's relation to a Dispatch Operating Point (DOP) such that a 'down' regulation occurs when the set point is less than the DOP, and an 'up' regulation occurs when the set point is equal to or larger than the DOP. As described in [16], a DOP is the trajectory a controlled unit is expected to follow in response to a dispatch command. Additionally, a Dispatch Operating Target (DOT) is an optimal dispatch based on telemetry which is also a single point on the DOP trajectory. As optimal dispatch is beyond the scope of this paper, we have defined DOP and DOT to be the median value of the AGC dispatch for the entire 15 minute simulation. This choice results in a relatively even split of up and down regulation classifications.

The first step in calculating a PS from simulated data involved down sampling the power output data p from a time step of 25×10^{-6} seconds to 1×10^{-3} seconds. The data was then grouped into dispatch segments τ of four seconds (i.e. t = 0.0-3.999, 4.0-7.999, etc.) such that the total number of τ comprising one 15 minute market period T is 225. An average value was then calculated for all p values in each τ. Averaging was not required for set point data s as it is constant for each τ. Using these average valued τ, an instruction c, response r, and deviation d were calculated as

$$c = s - DOP \tag{1}$$

$$r = p - DOP \tag{2}$$

$$d = |c - r|. \tag{3}$$

For τ that were not involved in a particular regulation calculation, $c = r = 0$. This ensures that regulation up commands were not considered for regulation down calculations and vice versa. It is worth noting that c and r should be negative for down regulation and positive for up regulation situations.

The final step in calculating a PS involved comparing the total deviation, which will always be positive, and total instruction for the market period according to

$$PS_{up} = 100\% \times \frac{\text{MAX}\left(0, \sum_{\tau=1}^{T} c - \sum_{\tau=1}^{T} d\right)}{\sum_{\tau=1}^{T} c} \tag{4}$$

for regulation up, and

$$PS_{down} = 100\% \times \frac{\text{MIN}\left(0, \sum_{\tau=1}^{T} c + \sum_{\tau=1}^{T} d\right)}{\sum_{\tau=1}^{T} c} \tag{5}$$

for regulation down. The minimum or maximum selection in the numerator ensure that the resulting PS is always a positive number between 0 and 100%.

IV. Automatic Generation Control

Automatic Generation Control (AGC) is classified as a type of secondary frequency response that acts to correct area interchange and frequency error. As described in [17], an AGC routine is configured per control area to calculate an Area Control Error (ACE) that is then dispatched to generation resources. The generation resources that receive an AGC dispatch signal then act to return the system to nominal operating conditions. The block diagram in Fig. 2 shows how Reported and Smoothed (filtered) ACE is a combination of scaled frequency error and interchange error. The variable B in the block diagram represents frequency bias in MW/mHz that is set by each area with AGC. In this work, B is set to 1.0% max area generation capacity.

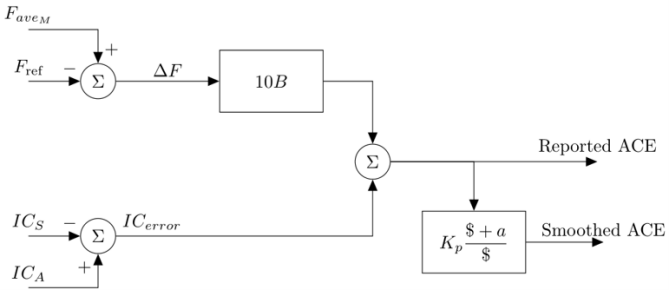

Fig. 2. Area control error block diagram.

All control areas calculate an inertia weighted frequency based on the machine speed and MVA rating of each rotating mass generator. This calculated frequency value is represented as F_{aveM} in Fig. 2. In a system with N generators, M areas, and N_M generators in area M, each area's total inertia H_{tot_M} and inertia weighted frequency F_{ave_M} are calculated by

$$H_{tot_M} = \sum_{i}^{N_M} MVA_{base_i} H_i \tag{6}$$

$$F_{ave_M} = \left(\sum_{i}^{N_M} Mach_{speed_i} MVA_{base_i} H_i \right) \frac{1}{H_{tot_M}}. \tag{7}$$

While other works dealing with AGC, such as [6] and [7], have continuously fed a dispatch signal to controlled assets, this work sends an updated signal every 4 seconds. This discrete signal approach is more in line with how utilities may actually send a dispatch signal to controlled resources and matches the behavior of real CAISO dispatch set points presented in [14].

A. Flexpower Plant Level Dispatch Control

While the system-wide AGC signal described in the previous section is sent every 4 seconds, the Flexpower plant was simulated with two different plant level control strategies. The first control strategy, referred to as CTRL A, acted every 2 seconds. This allowed for any remaining error from the first plant level dispatch in every τ to be adjusted with the second dispatch. The other control, CTRL B, was similar to CTRL A, but acted every 0.5 seconds. The goal of both strategies was to make a low-pass filtered positive sequence electric power

signal match the received area AGC dispatch signal while controlling the BESS to account for any variability introduced by changing resource levels.

V. Test Case Descriptions

To explore how a Flexpower plant may affect the PBR metric described in Section III, a 15 minute simulation was executed where real dispatch information (originally presented in [15]) was used to modulate a single load in each area. The three load modulation profiles are shown in Fig. 3. All profiles were scaled such that the maximum change was 40 MW as this was the largest variance seen in the original selection of data.

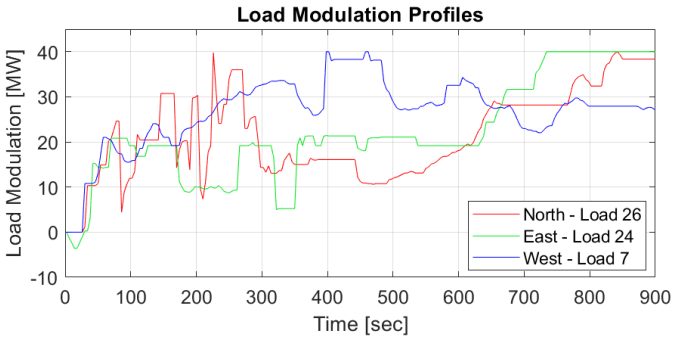

Fig. 3. Modulation profiles for controlled load in each area.

Using the load profiles shown in Fig. 3, four test cases were considered: A conventional only base case, a Flexpower case, and two Flexpower with variable resources cases. In all cases, AGC for each area was dispatched every four seconds with the ACE filter constants of Kp and a shown in Fig. 2 being 0.5 and 0.025, respectively. This gain and time constant were chosen to prevent system oscillations that could arise from a more aggressive dispatch.

A. Base Case

The base case simulated all generation in the IEEE 39 bus system using conventional steam turbines and governors connected to synchronous machine models. This was meant to provide simulated data of typical PBR metrics to compare with Flexpower case results.

B. Flexpower Case

In the first Flexpower case, G10 was replaced with a Flexpower plant that experienced constant wind and irradiance conditions. The slower control strategy, CTRL A, was used for internal plant dispatching. The removal of G10 affected how the North area frequency was calculated as only G8 and G9 were considered. Additionally, performance metrics refer to measuring mechanical power output, however, IBRs do not typically report mechanical power. Instead, the positive sequence power was calculated for the Flexpower plant at the point-of-common-coupling to the rest of the system and processed through a low-pass filter to remove high frequency oscillations. Filtering was also required for interchange measurements used in AGC calculations as the oscillations introduced by the Flexpower plant were seen system-wide.

C. Flexpower with Variable Resources Cases

The final two cases were the same as the Flexpower case with the addition of a Variable Resource (VR) profile for wind speed. The 10 minutes of wind data from [18] was doubled to fill the 15 minute simulation. The resulting wind speed profile with a time step of 1 second is shown in Fig. 4. Internal Flexpower plant CTRL A and CTRL B were utilized for these cases.

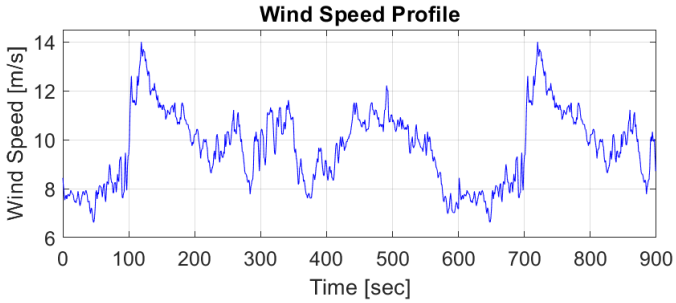

Fig. 4. Wind speed profile used in VR cases.

VI. Results

A. System Response

Fig. 5 shows the frequency of swing generator G2 for all cases remained roughly within +/- 30 mHz of nominal. More frequency activity was seen during the VR case using the slower Flexpower CTRL A. This was likely due to the governor action of G2 reacting to the variable output from the Flexpower plant.

Fig. 5. Swing generator frequency.

Fig. 6 presents the real power output of the WT and the BESS for all Flexpower cases over the course of the 15 minute simulation. In the first Flexpower case (solid blue line), the WT output remains constant while the BESS handles all AGC dispatches. In both VR cases, the BESS was also tasked with providing any additional power the WT may not have been able to provide due to wind speed variability.

Fig. 7 provides a detail view of the WT and BESS power output from $t = 80$ to $t = 100$. This figure is meant to show how the two VR cases responded to the variable WT power output. Specifically, how the faster CTRL B acts to smooth, or

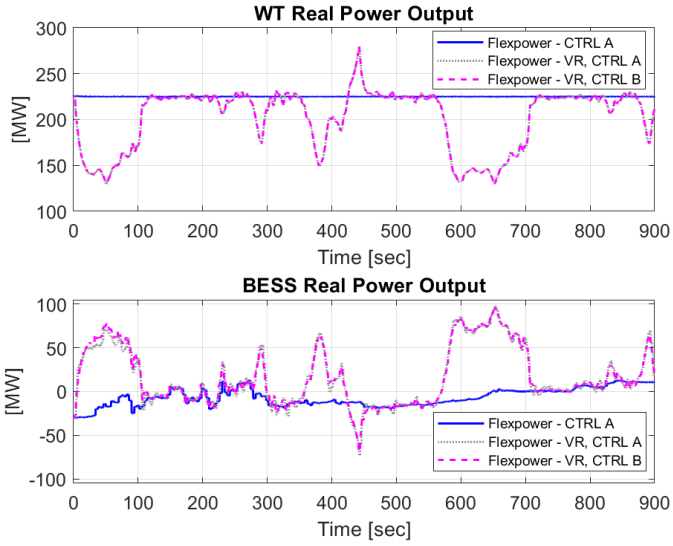

Fig. 6. Simulation results of WT and BESS real power output.

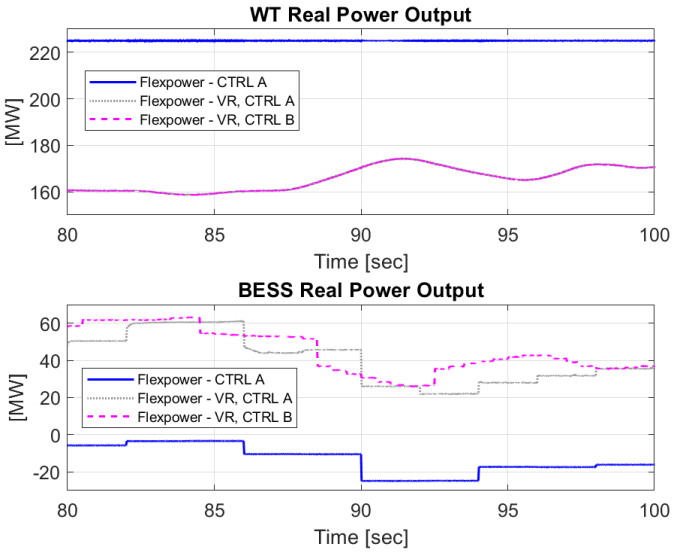

Fig. 7. Detail simulation results of WT and BESS real power output.

flatten, the variability introduced by the WT more accurately than CTRL A.

Fig. 8 depicts a detail view of the simulation outputs used to calculate the PS in the constant resource cases. It can be seen that the base case mechanical power slowly approached each new set point every 4 seconds and the average telemetry was typically calculated near the midway point between each dispatch. The Flexpower CTRL A case showed a much faster response when the internal plant controller acted every 2 seconds. As expected, the first dispatch contained error that the second dispatch attempted to correct.

Fig. 9 presents the same detail time range as Fig. 8 for the VR Flexpower cases. It can be seen that the electric power signal (Pe) under CTRL A noticeably drifted away from the desired set point as the variable resource changed between each internal dispatch of 2 seconds. Results from CTRL B, having an internal dispatch of 0.5 seconds, followed the desired dispatch much closer but still had error in the very first dispatch of each τ.

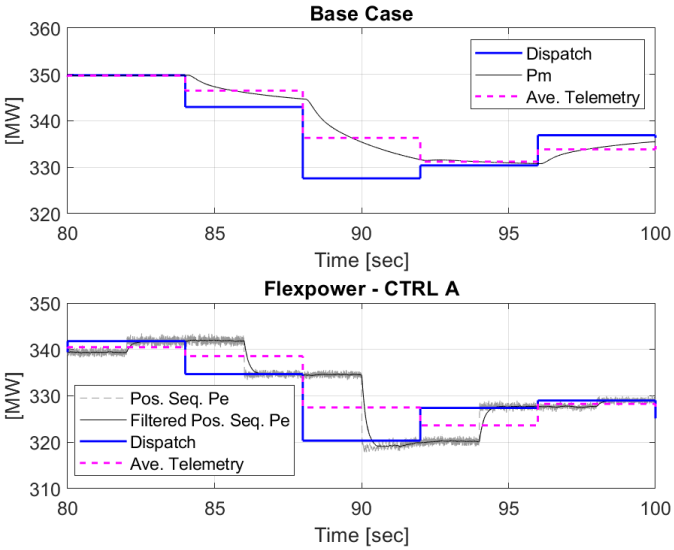

Fig. 8. Detail simulation results of dispatch following for the base case and constant resource Flexpower case.

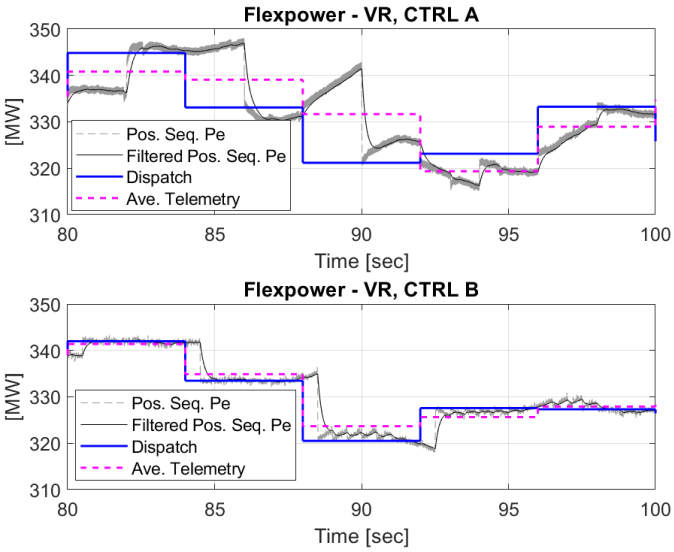

Fig. 9. Detail simulation results of dispatch following for variable resource Flexpower cases.

B. *Performance Score Results*

The calculated PSs for each area's regulation up and down are shown in Tables IV and V. The conventional base case PSs ranged from 83.50% to 96.47%. When resources were constant, Flexpower CTRL A improved the PS for the North in both regulation categories, but negatively affected the East and West areas regulation down by 0.45% to 1.46%. Mixed results from this case were seen in regulation up PSs as the East area increased by 0.16% while the West area decreased by 0.77%. When CTRL A was tasked with handling variable resources, all areas had lower PSs - especially in the North where the reduction in PS was 21.21% and 25.60% for the up and down regulation, respectively. The faster CTRL B handled the VR case better than CTRL A and resulted with improved PSs in all areas. Most notable was the 3.10% and 5.14% increase in PS for the North area.

TABLE IV
REGULATION UP PERFORMANCE SCORES.

Scenario	Area					
	North	Δ	East	Δ	West	Δ
Conventional Base Case	90.49	-	96.47	-	86.49	-
Flexpower - CTRL A	91.07	0.58	96.63	0.16	85.73	-0.77
Flexpower - CTRL A, VR	69.28	-21.21	94.71	-1.76	77.86	-8.63
Flexpower - CTRL B, VR	93.59	3.10	96.69	0.22	88.12	1.63

TABLE V
REGULATION DOWN PERFORMANCE SCORES.

Scenario	Area					
	North	Δ	East	Δ	West	Δ
Conventional Base Case	83.50	-	87.71	-	88.86	-
Flexpower - CTRL A	86.41	2.91	87.26	-0.45	87.40	-1.46
Flexpower - CTRL A, VR	57.90	-25.60	85.51	-2.19	81.58	-7.28
Flexpower - CTRL B, VR	88.64	5.14	88.43	0.72	89.36	0.50

VII. CONCLUSION

This paper presented the simulated impact of a single Flexpower plant on a PBR market metric using a modified IEEE 39 bus system, two internal plant control approaches, and variable generation resources. Simulations showed that despite very similar frequency characteristics between all cases, the calculated PSs may vary greatly. When resources were constant, the Flexpower plant improved the PS of its own area and had minor mixed effects on connected areas. The 2 second control employed by CTRL A did not respond fast enough to handle VR adequately, and consequentially, performance scores for all areas decreased. The 0.5 second internal plant control, CTRL B, responded to VR much better than CTRL A, and as a result, had performance scores that were mostly similar to, but also better than base case results.

Overall, results showed that IBRs acting to flatten variable resources can improve PBR metrics, but require an adequately fast control. If the utilized control is not fast enough, PBR metrics for all connected areas may become worse. Future work involving the Flexpower plant concept is likely to combine previously presented controls (resource aware frequency response, synthetic inertia, AGC following), improved internal plant dispatch, and refined BESS SOC handling.

REFERENCES

[1] Federal Energy Regulatory Commission (FERC), "Order No. 755," Tech. Rep., 2011.

[2] D. Littell, C. Kadoch, P. Baker, R. Bharvirkar, M. Dupuy, B. Hausauer, C. Linvill, J. Migden-Ostrander, J. Rosenow, W. Xuan, O. Zinaman, and J. a. Logan, "Next-Generation Performance-Based Regulation," NREL, Tech. Rep., 2017.

[3] F. Wilches-Bernal, T. Haines, R. Darbali-Zamora, and M. Jiménez-Aparicio, "A Resource Aware Droop Control Strategy for a PV, Wind, and Energy Storage Flexible Power (Flexpower) Plant," pp. 1–5, 2022.

[4] T. Haines, F. Wilches-Bernal, R. Darbali-Zamora, and M. Jiménez-Aparicio, "Flexible Control of Synthetic Inertia in Co-Located Clusters of Inverter-Based Resources," pp. 1–6, 2022.

[5] T. Athay, R. Podmore, and S. Virmani, "A Practical Method for the Direct Analysis of Transient Stability," pp. 573–584, 1979.

[6] D. M. Andrade, S. Gamboa, and J. A. Torres, "Distributed load-frequency control in power systems," in *2020 IEEE ANDESCON*, 2020, pp. 1–6.

[7] Y. Xu, C. Huang, X. Li, and F. Li, "A novel automatic generation control for thermal and gas power plants," in *2018 IEEE Power Energy Society General Meeting (PESGM)*, 2018, pp. 1–5.

[8] Y. Zuo, F. Sossan, M. Bozorg, and M. Paolone, "Dispatch and Primary Frequency Control with Electrochemical Storage: a System-wise Verification," 2018.

[9] A. Yazdani Iravani, Reza.,, "Voltage-sourced converters in power systems modeling, control, and applications," Hoboken, N.J., 2010. [Online]. Available: http://www.books24x7.com/marc.asp?bookid=35181

[10] K. Clark, N. Miller, and J. Sanchez-Gasca, "Modeling of GE Wind Turbine-Generators for Grid Studies Prepared by," 2010.

[11] N. Miller, J. MacDowell, G. Chmiel, R. Konopinski, D. Gautam, G. Laughter, and D. Hagen, "Coordinated voltage control for multiple wind plants in Eastern Wyoming: Analysis and field experience," in *2012 IEEE Power Electronics and Machines in Wind Applications*, 2012, pp. 1–8.

[12] J. M. MacDowell, K. Clark, N. W. Miller, and J. J. Sanchez-Gasca, "Validation of GE wind plant models for system planning simulations," in *2011 IEEE Power and Energy Society General Meeting*, 2011, pp. 1–8.

[13] P. Pourbeik, S. E. Williams, J. Weber, J. Sanchez-Gasca, J. Senthil, S. Huang, and K. Bolton, "Modeling and Dynamic Behavior of Battery Energy Storage: A Simple Model for Large-Scale Time-Domain Stability Studies," *IEEE Electrification Magazine*, vol. 3, no. 3, pp. 47–51, 2015.

[14] CAISO, "Pay for performance mileage example," www.caiso.com/Documents/PayForPerformanceMileageExample.xls, 2011, accessed: 2022-06-14.

[15] A. Sadeghi-Mobarakeh and H. Mohsenian-Rad, "Performance Accuracy Scores in CAISO and MISO Regulation Markets: A Comparison Based on Real Data and Mathematical Analysis," pp. 3196–3198.

[16] California ISO, "Technical Bulletin 2009-06-05," CAISO, Tech. Rep., 2009.

[17] North American Electric Reliability Corporation (NERC), "Balancing and Frequency Control: A Technical Document Prepared by the NERC Resources Subcommittee," pp. 1–53.

[18] F. Wilches-Bernal, J. H. Chow, and J. J. Sanchez-Gasca, "A fundamental study of applying wind turbines for power system frequency control," *IEEE Transactions on Power Systems*, vol. 31, no. 2, pp. 1496–1505, 2016.